RSC Advances

PAPER

View Article Online
View Journal | View Issue

Cite this: *RSC Adv.*, 2020, **10**, 1603

Improving the toughness of thermosetting epoxy resins *via* blending triblock copolymers

Lei Tao,[ac] Zeyu Sun,*[abc] Wei Min,[ac] Hanwen Ou,[ac] Liangliang Qi[ac] and Muhuo Yu*[abc]

In this study, the triblock copolymer poly(methyl methacrylate)-*b*-poly(butyl acrylate)-*b*-poly(methyl methacrylate) (MAM) was used to modify bisphenol A epoxy resin to improve its toughness. The effects of MAM on the curing behaviors, mechanical properties, fracture morphology and thermal properties of epoxy were carefully studied. The results of dissolution experiments show that MAM has good compatibility with epoxy resin under certain conditions. FT-IR and DSC analyses show that adding MAM to epoxy hinders the curing reaction of epoxy resin, without participating in the curing reaction and changing the curing mechanism. The mechanical properties indicated by K_{IC} and impact strength with an MAM content of 10 phr for the toughened system increase by 91.5% and 83.5%, respectively, compared to the situation without MAM, which may ascribed to the nanoparticles formed during the process of MAM/epoxy blending. In the curing process of an epoxy resin, the typical phase structure that occurs through the self-assembly process can be clearly observed in the MAM/epoxy blends. As the MAM content increases, the amount of nanoparticles gradually increases. This work further confirms that the toughness of the composite material was enhanced to a large extent without significantly decreasing the glass transition temperature of the blends.

Received 6th November 2019
Accepted 16th December 2019

DOI: 10.1039/c9ra09183a

rsc.li/rsc-advances

1. Introduction

Epoxy resin (EP) has been widely used in aerospace, rail transportation, wind power, automobiles and other related fields owing to its outstanding bonding performance, favorable mechanical properties, low shrinkage and excellent chemical stability.[1–3] However, because of a high degree of cross-linking, internal stress, great brittleness and poor impact resistance after curing, its application has been greatly hindered in many areas, especially in high-tech fields. Therefore, an improvement in the toughness of epoxy resin to broaden its applications has attracted more and more attention in recent years.[4–6]

Quite a large number of studies in the literature have shown that the addition of a toughening agent is a simple and effective way to improve the toughness of epoxy resin. Among these studies, reactive functionalized liquid rubber has made great progress in the modification of epoxy resin. Conventionally used reactive functionalized rubbers include carboxyl terminated butadiene acrylonitrile (CTBN),[4,7,8] amine terminated butadiene acrylonitrile (ATBN),[9,10] and epoxy terminated butadiene acrylonitrile (ETBN).[11] However, the decrease in glass transition temperature and modulus severely limits the range of application of rubber-based epoxy resin.

In recent years, nanostructured thermosetting resins have been obtained through blending a block copolymer (BCP) with a fine structure with an epoxy resin. The notch toughness of the resin has been greatly enhanced while the elastic modulus and glass transition temperature remain unchanged.[12–22] Frequently-used thermoplastics include poly(methyl methacrylate)-*b*-poly(butyl acrylate)-*b*-poly(methyl methacrylate) (PMMA-*b*-PnBA-*b*-PMMA, MAM),[22] poly(ethylene oxide)-*b*-poly(ethyl propylene) (PEO-PEP),[21] and poly(ethylene oxide)-*b*-poly(ε-caprolactone) (PEO-*b*-PCL).[20] BCPs, as amphiphilic molecules, can form micellar structures *via* self-assembly and can be effectively used as nano-toughers for epoxy resins. The formation of nanostructures of block copolymers in epoxy resins originates from the difference in compatibility of the different building blocks in the matrix, which requires a block copolymer with at least one epoxy-miscible block and one epoxy-immiscible block in the molecular structure. In epoxy resins, constructed micro/nanostructures take the form of different morphologies, such as spherical micelles, wormlike micelles or vesicles, depending on the molecular weight, block length and composition of the BCPs. With the addition of a relatively small amount of BCPs (≤5 phr), the fracture toughness of the resins can be significantly improved.[13,16,18,21] Poly(methyl methacrylate)-*b*-poly(butyl acrylate)-*b*-poly(methyl methacrylate) (MAM) is a typical amphiphilic block copolymer, which has been used to research

[a]*State Key Laboratory for Modification of Chemical Fibers and Polymer Materials, College of Materials Science and Engineering, Donghua University, Shanghai 201620, China. E-mail: yumuhuo@dhu.edu.cn; Tel: +86-139-0715-9052*

[b]*Shanghai Key Laboratory of Lightweight Structural Composites, Donghua University, Shanghai 201620, China*

[c]*Center for Civil Aviation Composites, Donghua University, Shanghai 201620, China*

the relationship between the phase structure and toughness of cured epoxy resin. Barsotti *et al.*[31] compared the fracture toughness improvement ability of a block copolymer and CTBN in the same epoxy system but used another block copolymer: MAM. These researchers reported that MAM modified epoxies have a significantly higher fracture toughness than CTBN modified epoxies on addition of the same wt% loading. They reported that, for example, in a dicyandiamide (DICY) cured DGEBA epoxy, 5 wt% MAM modified epoxy gave a value of $K_{IC} =$ 1.64 MPa $m^{1/2}$ while a value of $K_{IC} =$ 1.32 MPa $m^{1/2}$ was measured for a 5 wt% CTBN modified epoxy. Wang *et al.*[30] mixed MAM and CSP as a toughening agent for epoxy resin. Their results indicated that when 3 phr MAM and 5 phr CSP were added, the fracture toughness of the MAM/CSP/epoxy resin composites was increased by 91.4% while the mechanical properties of the composites were not lost. However, a few reports have emphasized the influence of MAM on the curing behavior of epoxy resin, which may lead to a change in phase structure and mechanical properties after curing.

In this work, modification of bisphenol A epoxy resin was obtained with an MAM triblock copolymer as the toughening agent. The curing kinetics of the MAM/epoxy blend system was studied systematically, and the curing mechanism of the epoxy resin blend system in the presence of MAM was analyzed. The results show that the addition of MAM does not change the curing reaction or curing mechanism of the epoxy resin. In the epoxy system, the amphiphilic copolymer absorbs external energy by different phase separation structures which were constructed by self-assembly, which effectively improves the mechanical properties of the resin. What is more, our research also shows that MAM has little effect on the glass transition temperature of the system under conditions which produce a better toughening effect.

2. Experimental

2.1. Materials

Triblock copolymer MAM was purchased from Shanghai Huayu New Materials Technology Co., Ltd. Bisphenol A epoxy resin (E51) with an epoxy equivalent of 182–192 g mol^{-1}, was obtained from Nanya Plastics Industry Co., Ltd. The curing agent was dicyandiamide (DICY), supplied by the Shenzhen Jiadida New Material Technology Co., Ltd. The accelerator was 1,1′-(methylenebis(4,1-phenylene))bis(3,3-dimethylurea) (UA23), which was purchased from Shanghai Huayu New Materials Technology Co., Ltd.

2.2. Preparation of the MAM/epoxy blends

Firstly, the MAM particles were dissolved in the epoxy resin at 150 °C until the mixed system had completely clarified. After the temperature had decreased to 80 °C, the reaction system was mixed with DICY and UA23 in a three-roller mill three times. Finally, the mixture was defoamed in a vacuum oven at 100 °C until the bubbles were completely discharged. The mixture was transferred to a mold coated with a release agent and then the model was kept at 120 °C for 2 h. After cooling and demolding, the cured product of an MAM/epoxy composite was obtained. According to the different weight ratios of MAM to epoxy resin, the samples were recorded as 0, 5, 10, 15, and 20 phr. Table 1 shows the chemical compositions and Fig. 1 shows a flow diagram of preparing an epoxy resin sample.

2.3. Characterization

A hot stage polarizing microscope was used to observe the dissolution of MAM in epoxy resin (LINKAM TMS94 hot stage and Olympus BX5 optical microscope). Fourier transform infrared spectroscopy (FT-IR) was applied to investigate the curing reaction. The FT-IR spectra of the samples were recorded with a Nicolet 6700 FT-IR spectrometer with a smart-ATR attachment. The viscoelasticity of the MAM/epoxy blends was tested using dynamic mechanical analysis (DMA, TA Q800). Rectangular specimens of 60 mm × 13 mm × 3 mm were prepared for DMA analysis, on a 3-point flexural mode at a frequency of 3 Hz and heated from 50 °C to 250 °C.

The tensile and flexural properties of the blends were tested according to the ASTM D638-10 and D5045-14 standards, respectively. For a typical flexural strength and modulus test, the specimen dimensions were 127 mm × 12.7 mm × 3.2 mm. The fracture toughness of the MAM/epoxy blends was determined by a single-edge notched 3-point flexural test (SENB) according to ASTM D5045-14. Rectangular specimens of 44 mm × 10 mm × 5 mm with a 5 mm long notch were prepared for measurement. A WANCE 203 B-TS micro computer controlled electromechanical universal testing system was applied to perform these measurements.

The critical stress intensity factor (K_{IC}) was adopted to inquire into the mechanical interfacial properties or the fracture toughness of the epoxy/MAM blends. The value of K_{IC} is determined based on the ASTM D5045-14 standard as follows:

$$K_{IC} = \left(\frac{P}{Bw^{1/2}}\right) f(x)$$

where P is the loading weight, B is the thickness of the specimen, w is the depth (width) of the specimen, a is the crack length, x is the ratio of the crack length to the depth of specimen, a/w, and $f(x)$ is the calibration factor, which is represented as follows:

$$f(x) = 6x^{1/2}\frac{[1.99 - x(1-x)(2.15 - 3.93x + 2.7x^2)]}{(1-2x)(1-x)^{3/2}}$$

Izod pendulum impact tests (JINYANG XJJUD-50Q) were performed based on ASTM D256-10 standard under an impact

Table 1 Weight ratio of E51/MAM/DICY/UA23 blends

Weight ratio (%)	0 phr	5 phr	10 phr	15 phr	20 phr
E51	100	100	100	100	100
MAM	0	5	10	15	20
DICY	7	7	7	7	7
UA23	1.5	1.5	1.5	1.5	1.5

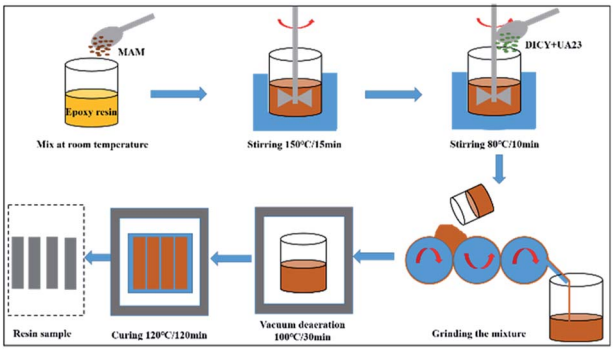

Fig. 1 The flow diagram of preparing an epoxy resin sample.

speed and impact energy of 3.5 m s^{-1} and 5.5 J, respectively. The sample sizes was 63.5 mm × 12.7 mm × 6.35 mm and each sample had a constant notch.

The fractured surfaces of the cured MAM/epoxy blends were analyzed in detail by a Hitachi SU8010 scanning electron microscope (SEM) system and an Atomic Force Microscope (AFM).

The thermal stability of the cured MAM/epoxy blends was studied with a Netzsch TG 209 F1 Iris thermogravimetric analyzer. The samples were heated from room temperature to 800 °C at a heating rate of 10 °C min^{-1} in a nitrogen atmosphere.

3. Result and discussion

3.1. Solubility

The compatibility of toughened materials with resins has a significant impact on the processing of the resins. In order to study the compatibility of the epoxy resin and MAM, a hot stage polarizing microscope was used to observe the dissolution of MAM in the resin, and the results are shown in Fig. 2. It can be observed that MAM was completely dissolved within 15 min at 150 °C. In addition, the dissolution system was completely transparent and no other impurities were produced. These phenomena indicate that MAM can achieve good stability in epoxy resin in a very short time.

3.2. Curing kinetics of MAM/epoxy resin blends

The performance of the cured epoxy resin was highly dependent on the crosslinked network structure of the epoxy resin. The formation of the crosslinked network structure of the thermosetting resin was closely related to the curing reaction kinetics. Therefore, DSC was used to analyze the effect of MAM on the curing behavior of epoxy resin, as shown in Fig. 3. The curing of epoxy resin is an exothermic process. Fig. 2 indicates that the MAM/epoxy resin system has a distinct curing exothermic peak between 100 °C and 220 °C for blending with the same MAM content. The peak temperature (T_p) of the solidification curve gradually increases as the heating rate in an MAM/epoxy resin system increases. Moreover, the shape of the exothermic peak gradually becomes sharp. The blended systems show a similar trend with the addition of different contents of MAM. The main reason is that the exothermic hysteresis of the curing reaction gradually increases and the temperature difference generated by the reaction becomes larger as the heating rate increases. Therefore, the peak of the exothermic heat of the curing reaction moves toward high temperature.

The apparent activation energy (ΔE) and reaction order (n) are important kinetic parameters in the curing of epoxy resin, and also are the theoretical basis for the formulation of process parameters and process control of epoxy resin curing. ΔE directly reflects the difficulty of the curing reaction, and can be calculated according to the Kissinger method,[23] as shown in formula (1). The reaction order (n) reflects the complexity of the reaction and can be used to estimate the curing reaction mechanism, which can be based on the Crane equation[24] calculated as shown in formula (2).

$$\frac{d\left(\ln \beta / T_p^2\right)}{d\left(1/T_p\right)} = -\frac{\Delta E}{R} \quad (1)$$

$$\frac{d(\ln \beta)}{d\left(1/T_p\right)} = -\frac{\Delta E}{nR} + 2T_p \quad (2)$$

where β is the heating rate, T_p is the peak temperature, R is the ideal gas constant which is 8.314 J (mol^{-1} K^{-1}), and ΔE is the activation energy, and n is the order of the reaction.

According to the Kissinger and Crane equations, the peak temperature (T_p) of the MAM/epoxy system with different MAM contents at different heating rates β was substituted into formulas (1) and (2). After that, $\ln(\beta/T_p^2)$ and $\ln \beta$ were plotted as a function of $1000/T_p$, as shown in Fig. 4(a) and (b), respectively. The slope of each fitted line is obtained by the linear regression method. The complex correlation coefficients R^2 of the two linear fittings all reach 0.99 or higher, indicating an excellent fit.

The values of ΔE and n are calculated based on eqn (1) and (2), as shown in Table 2. It was found that the values of ΔE have two different stages with an increase in MAM content in the blended system. The activation energy of the reaction of the blended system will not change when the content of MAM is less than 10 phr, but the activation energy of the blend increases sharply when it reaches 10 phr. However, with the addition of MAM, the activation energy of the resin system remains stable. A lower content of MAM in the blended system has little effect on the viscosity. Nevertheless, the viscosity of the system increases sharply when the MAM content of the blended system is over 10 phr. The probability of the epoxy resin reacting with the curing agent was hindered by the MAM polymer chain. Difficulty in the reaction of the blended system leads to a decrease in the rate of the curing reaction, which was manifested by an increase in apparent activation energy. Moreover, as evident from Table 1, the reaction order (n) of each system is stable between 0.92 and 0.93, demonstrating that the addition of MAM will not change the curing reaction mechanism of the epoxy resin.

3.3. FT-IR analysis

Various outstanding properties of epoxy resins are obtained through their fully crosslinked structures. Therefore, in order to

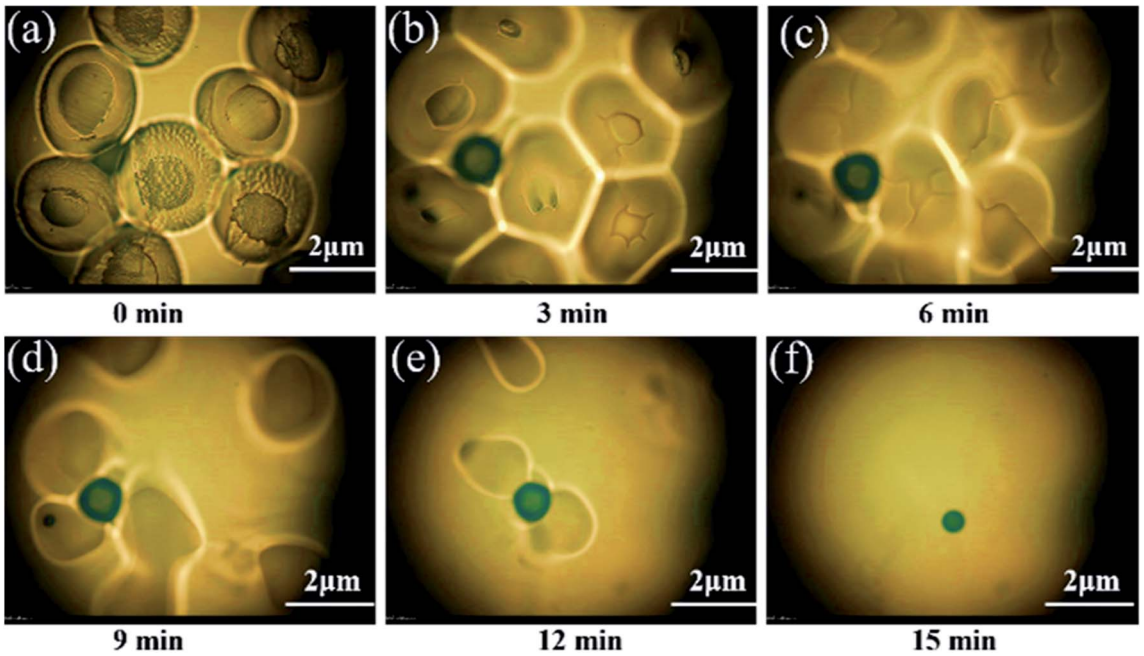

Fig. 2 The dissolution process of MAM particles in epoxy resin at 150 °C, followed by optical microscopy (a) 0 min, (b) 3 min, (c) 6 min, (d) 9 min, (e) 12 min, (f) 15 min.

study the influence of MAM on the chemical structure of cured epoxy resin, FT-IR analysis was conducted to study the completion of the curing reaction. Fig. 5 shows the infrared spectra of the MAM/epoxy blends. The epoxy absorption peak at 915 cm^{-1} completely disappears after curing, indicating that the epoxy resin curing reaction was complete. This phenomenon indicates that the addition of MAM would not affect the curing reaction of epoxy resin.

3.4. Mechanical properties

In order to study the effect of the addition of MAM on the mechanical properties of the blends, the tensile strength, tensile modulus, flexural loudness, flexural modulus, fracture toughness and impact strength were studied. The results are shown in Fig. 6–8. Fig. 6(a–c) shows the tensile properties of blends with different MAM contents. Unfortunately, both tensile strength and tensile modulus

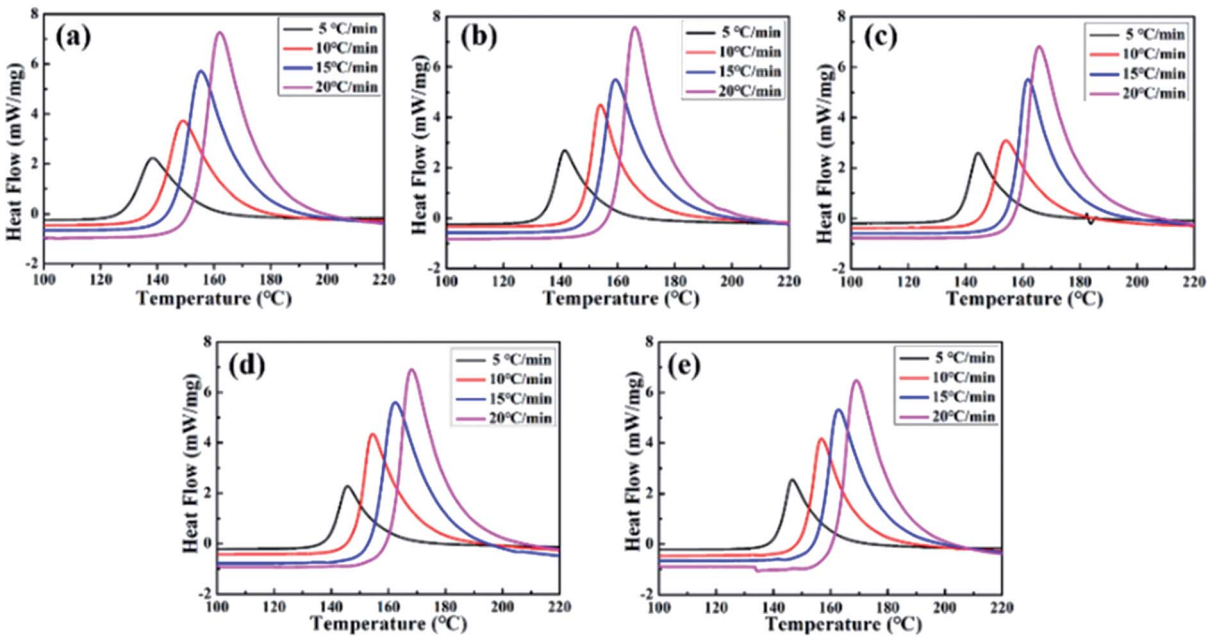

Fig. 3 DSC curves of MAM/epoxy systems at different heating rates of the sample (a) 0 phr, (b) 5 phr, (c) 10 phr, (d) 15 phr, and (e) 20 phr.

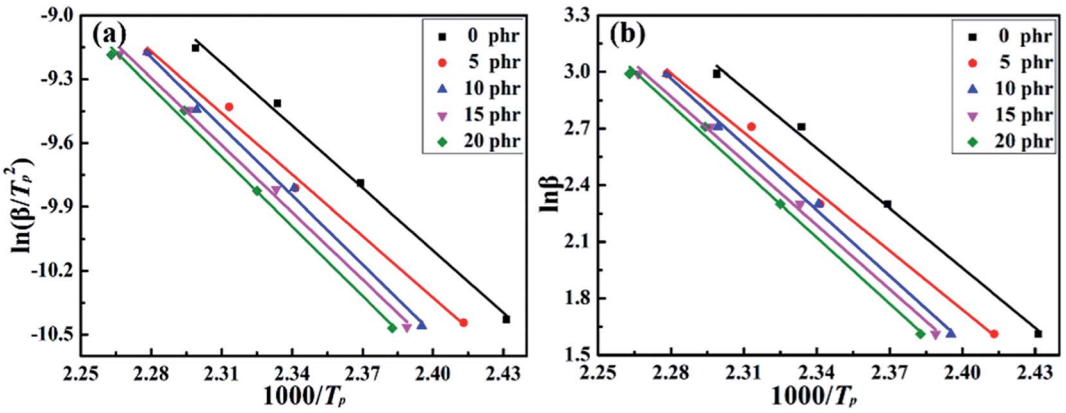

Fig. 4 Plots for determining the activation energy of the curing reaction by Kissinger equation (a) $\ln(\beta/T_p^2)$ *vs.* $1000/T_p$, (b) $\ln \beta$ *vs.* $1000/T_p$.

decrease with the addition of MAM, and the tensile strength decreases significantly. When the addition amount is 20 phr, the tensile strength and modulus decrease by about 24.6% and 20.2%, respectively. In contrast, the elongation at break of the blended system increases significantly with an increase in the MAM content.

Fig. 7 show the flexural strength and flexural modules of MAM/epoxy blends. Regrettably, like tensile properties, both flexural strength and flexural modulus are reduced with the addition of MAM. It is clear that both the flexural properties of the cured MAM/epoxy blends are slightly reduced with an increase in MAM ratio. When the amount added reaches 20 phr, the flexural strength and flexural modulus have decreased by about 11.3% and 23.9%, respectively.

Fig. 8(a) and (b) shows the critical stress intensity factor and impact properties of MAM/epoxy blends. Interestingly, in contrast to the tensile and flexural properties, the addition of MAM does not reduce but improves the critical stress intensity and impact properties of the epoxy resin as the MAM content increases. Compared with pure epoxy resin, the fracture toughness and impact strength of all blended samples are significantly improved. When the MAM content was below 10% and the content of MAM was increased, the fracture toughness and impact strength of the blended system showed a large increase. However, at high MAM concentrations (15 phr and 20 phr), the toughness of the system was not significantly improved relative to the 10% content system.

3.5. Phase structures of the MAM/epoxy blends

The fracture morphology of the blended systems was observed by SEM to reveal the relationship between mechanical properties and internal structure, as shown in Fig. 9. In a micrograph of the 0 phr MAM/epoxy blend (Fig. 9(a)), the fracture surface of the epoxy resin appears as a smooth plane, as predicted, with no obvious defects, unfolding obvious brittle characteristics. In contrast, with the addition of MAM block copolymer into the epoxy resin, the morphology of the fracture surface of the epoxy resin blended system begins to roughen and the roughness increases with an increase in the content of MAM. Compared with the cured neat epoxy resin, the rough structure of these fracture faces was produced by the dispersed phase of the MAM modified epoxy resin blend. The 15–20 phr MAM modified cured blend [Fig. 9(d) and (e)] was found to have submicron-sized cavities. For all of the samples, as the triblock copolymer MAM content increased from 5 phr to 20 phr, the size of the inclusions increased.

AFM photographs of the cured blends in Fig. 6 clearly reveal the differences in surface fracture morphology. We note that there is only one phase in the pure epoxy (0 phr) with a smooth surface, as shown in Fig. 10(a). However, after the addition of MAM to the epoxy resin, an elliptical granular material

Table 2 Cure kinetic parameters and R^2 of MAM/epoxy systems with different MAM contents

Sample	0 phr	5 phr	10 phr	15 phr	20 phr
ΔE (kJ mol^{-1})	81.228	80.06	89.708	88.463	90.623
R_1^2	0.9936	0.9929	0.0046	0.0048	0.9947
n	0.923	0.921	0.928	0.927	0.930
R_2^2	0.9938	0.9915	0.9960	0.9953	0.9947

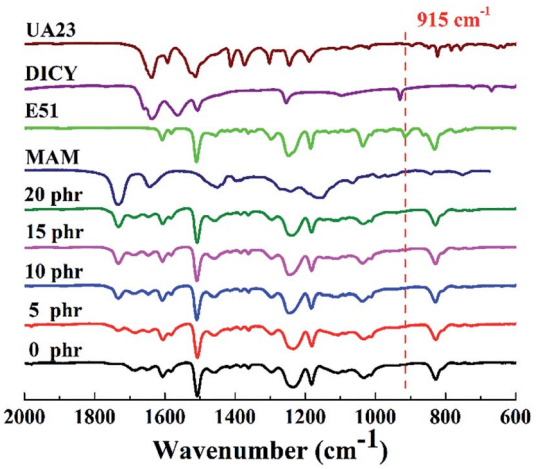

Fig. 5 FT-IR spectrum of epoxy resin (E51) before curing, the MAM/epoxy blends after curing with different MAM contents, MAM, DICY and UA23.

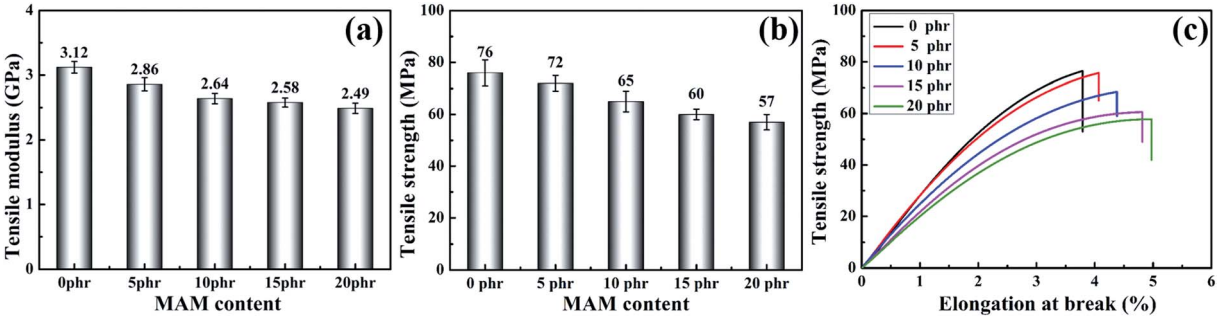

Fig. 6 The tensile modulus (a), tensile strength (b) and stress-elongation at break curves (c) of cured MAM/epoxy blends.

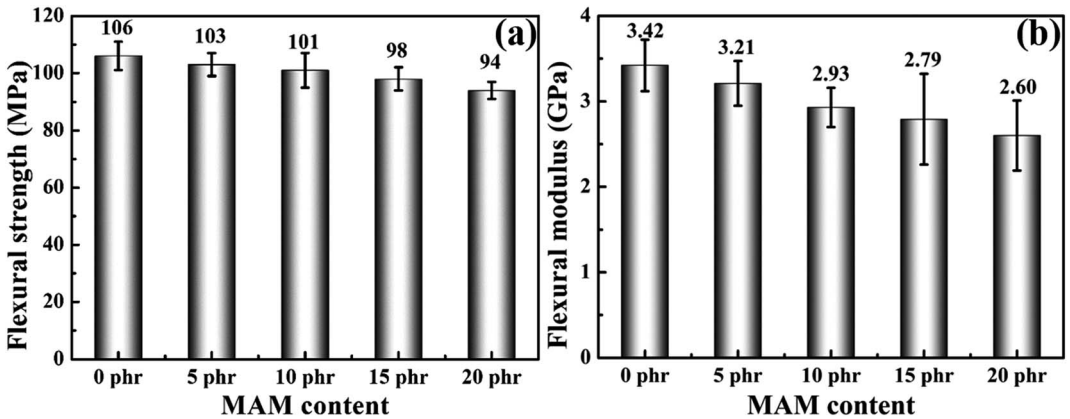

Fig. 7 The flexural strength (a) and flexural modulus (b) of cured MAM/epoxy blends.

appeared, as shown in Fig. 10(b) and (c), and the size and distribution density of the elliptical particles increased with an increase in the MAM content, and these particles represent part of the MAM. The epoxy block is such that the cured epoxy/MAM forms a two-phase structure. However, as the MAM content is increased to 15 phr, the epoxy-blocks are bonded to each other, exhibiting a bicontinuous phase, as shown in Fig. 10(d). With a further increase in the content of MAM to 20 phr, the elliptical particulate matter disappears and the surface becomes relatively smooth. This structure is shown in Fig. 10(e).

The nanostructured epoxy resin system is the result of a combination of self-assembly mechanisms.[25] Studies have shown that in the MAM-containing triblock copolymer system, the PBA sub-chain was first self-organized into a sphere according to the concentration of the triblock copolymer before the curing reaction. With an increase in the MAM content, the spherical size and number of PBA sub-chains formed by self-assembly gradually increased. However, the PMMA sub-chain was always compatible with the epoxy before and after curing. The formation process of the structure is shown in Fig. 11.

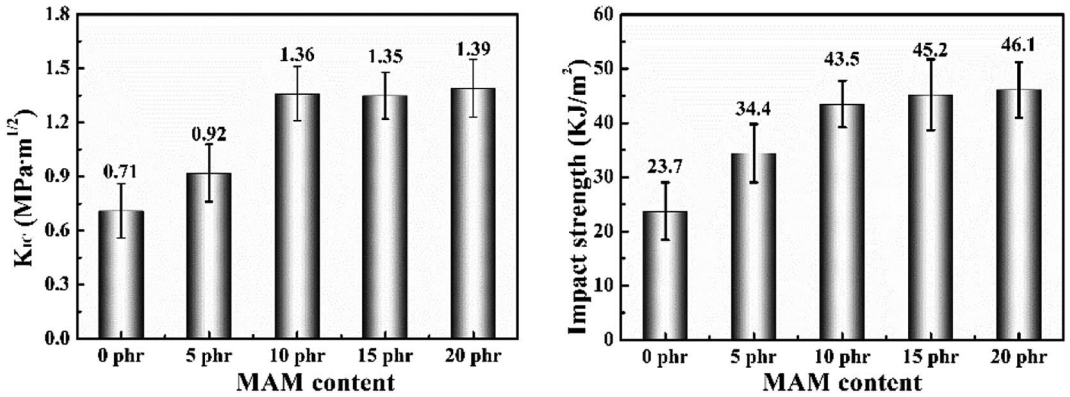

Fig. 8 The fracture toughness in terms of critical stress intensity factor (K_{IC}) and impact strength of the MAM/epoxy blends as a function of MAM content.

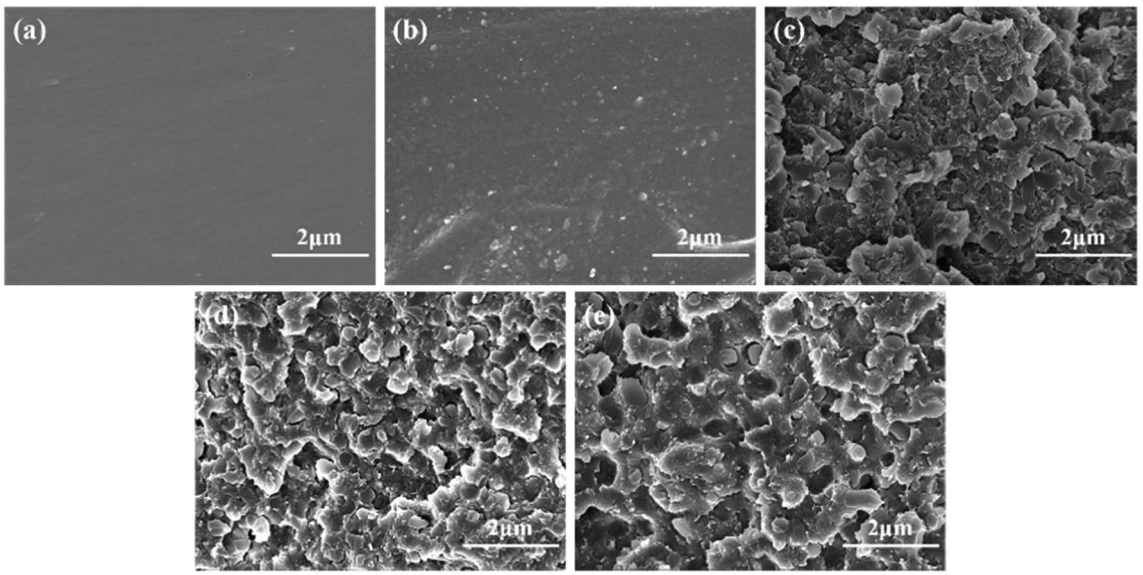

Fig. 9 SEM images of the fractured surfaces of the MAM/epoxy blends: (a) 0 phr, (b) 5 phr, (c) 10 phr, (d)15 phr, and (e) 20 phr.

According to the results shown in Fig. 6–8, some might speculate that the mechanical properties of the epoxy/MAM blend should correspond to the phase structure of the blend and the properties of the modified particles. The decrease in the tensile strength and modulus, and flexural strength and modulus with the introduction of MAM content, as shown in Fig. 6 and 7, might be the result of the tensile and flexural property being mainly influenced by the interaction between the epoxy networks, the crosslinking densities and the defects in the resin.[26] The addition of MAM reduces the crosslinking density of the epoxy resin and causes certain defects in the epoxy resin, regardless of the phase structure. On the other hand, the addition of MAM reduces the strong rigidity and internal friction of the network. The combination of the two causes the tensile bending property of the epoxy resin to decrease.

As shown in Fig. 10(b) and (c), the uniform dispersion of the MAM domains was considered to improve the fracture toughness, and the impact properties of the blend are improved by the bridging effect and the crack pinning effect.[27] Various toughening mechanisms, such as crack path deflection and matrix plastic deformation, can also be used to account for the increase in toughness of the blend.[28,29] The cured mixture of nanospheres and vesicles containing 5 phr and 10 phr MAM

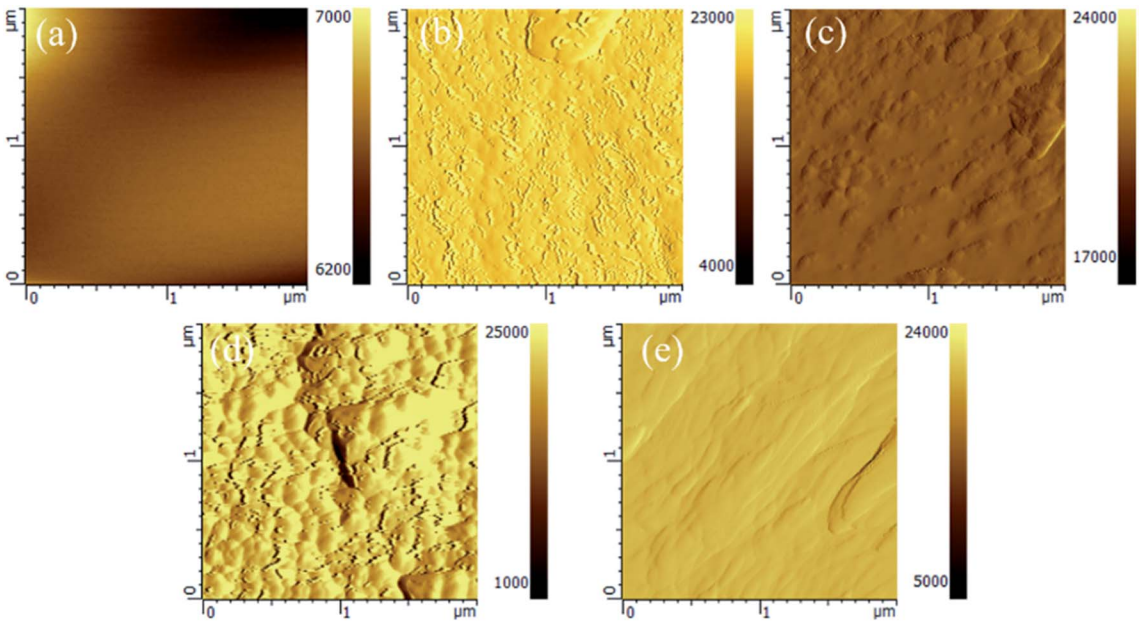

Fig. 10 AFM images of the fractured surfaces of the MAM/epoxy blends: (a) 0 phr, (b) 5 phr, (c) 10 phr, (d)15 phr, and (e) 20 phr.

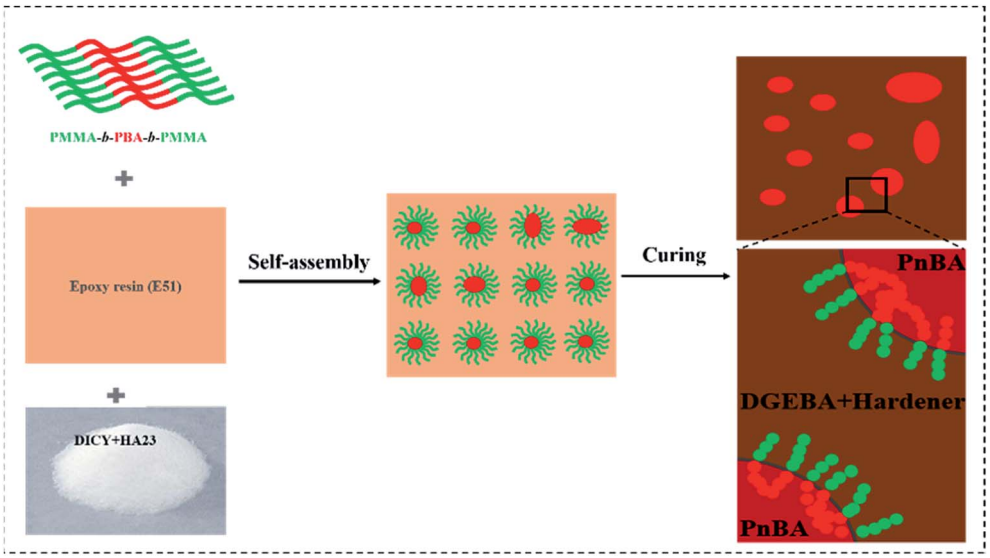

Fig. 11 Schematic diagram of BCP self-assembly during resin curing.

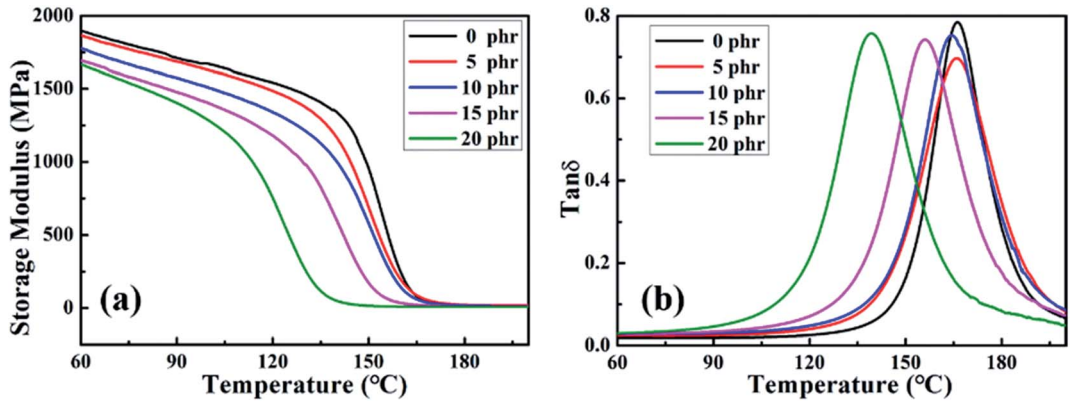

Fig. 12 Curves of (a) storage modulus E' and (b) tan δ with temperature of MAM/epoxy cured products containing different MAM contents.

increased K_{IC} by 29.6% and 91.5%, respectively. However, at high MAM concentrations (15 phr and 20 phr), complex inclusions did not produce a significant improvement in toughness. Larger particles act as defects, which can lead to premature failure of the matrix, thus reducing the overall toughness. These defects create some toughness. Therefore, it was observed that K_{IC} was only slightly increased by adding MAM contents of 10 phr and 20 phr.

3.6. Thermal properties

3.6.1. Dynamic mechanical thermal analysis. Dynamic mechanical thermal analysis (DMA) gives more insight into the viscoelastic properties and the morphologies of MAM/epoxy blends. The effect of temperature on the storage modulus of the cured MAM/epoxy blend is shown in Fig. 12(a). The results show that the storage modulus of the blend decreases with an increase in MAM content. The tan δ values of the MAM/epoxy blends are plotted against temperature in Fig. 12(b). The results present only one peak, which means that the blended system has only one glass transition temperature (T_g), and we also notice that T_g decreases as the content of MAM increases. The possible reason for these phenomena is that the storage

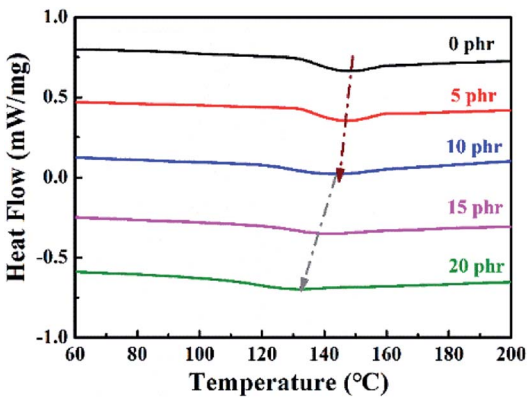

Fig. 13 DSC curves of MAM/epoxy cured products with different MAM contents.

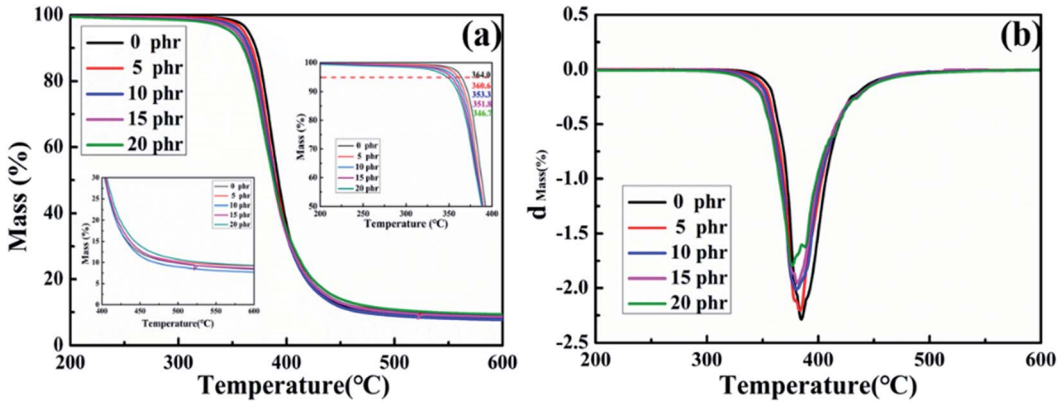

Fig. 14 Curves of thermogravimetric (a) and DTG (b) of MAM/epoxy cured products with different MAM contents.

modulus and glass transition temperature of the flexible block copolymer are lower than those of the pure epoxy resin system; in addition, the added MAM reducing the curing degree of the epoxy resin results in a decrease in the storage modulus and T_g of MAM/epoxy blends. However, the extent of the reduction in glass transition temperature of the blended system was not large, indicating that the block copolymer has little effect on the thermal properties of the blended system.

3.6.2. Glass transition temperature of MAM/epoxy cured product. In order to study the effect of MAM on the thermal properties of epoxy resin, DSC was used to analyze the glass transition temperature (T_g) of MAM/epoxy cured products with different MAM contents. As shown in Fig. 13, the addition of MAM did not increase but decreased the T_g of the epoxy resin. Generally, the T_g of cured epoxy depends on its chain flexibility, crosslinked structure and the intermolecular hydrogen bonding interaction of the composites. With the addition of MAM, the flexible segments would soften the crosslinked structure, so the T_g of modified epoxy resins would decrease. At the same time, the addition of MAM increases the viscosity of the system, resulting in incomplete curing reactions. Therefore, the T_g of the MAM/epoxy composite is lower than the T_g of pure epoxy. The results of the DSC curves are very consistent with the DMA results.

3.6.3. Thermogravimetric analysis. The thermal stability of the cured MAM/epoxy blends was analyzed by thermogravimetric analysis. The thermogravimetric results are shown in Fig. 14. Only one decomposition step of the MAM/epoxy resin blends was found in the range from 200–600 °C, indicating that MAM and epoxy resin have good compatibility. Observing the DTG curves in Fig. 14(b), we can see that with an increase in BCP content, the maximum decomposition rate of the blended system moves in the low-temperature direction. By analyzing the starting point T_{d5} of the thermal decomposition temperature of five different BCP additions, we found that the decomposition starting temperature of the epoxy resin composites is within the range 345–365 °C, and the decomposition starting temperature gradually decreases with a gradual increase in BCP content, so the initial temperature is reduced by 17.3% compared to that of pure epoxy resin. It can be speculated that a possible reason is that the crosslinking density of the epoxy resin may decrease due to the addition of MAM, resulting in a decrease in the thermal decomposition temperature of blended system. Through an analysis of the amount of residual carbon, we found that the amount of residual carbon produced in the final stage of the decomposition of the blend was 10 phr, and the overall results show an increasing trend. The ratios for 10 and 15 phr had decreased, which may be related to the phase structure of the material.

4. Conclusions

In general, an amphiphilic block copolymer MAM was incorporated to improve the toughness of epoxy resin. The solubility of MAM in epoxy resin and the effect of MAM on the curing reaction of epoxy resin, mechanical properties, phase structure and thermal properties were studied. Dissolution experiments showed that MAM has good solubility in epoxy resin and can be well dissolved in it to prepare MAM/epoxy blends. The DSC results showed that the addition of MAM does not change the curing mechanism but hinders the curing of the epoxy resin. FT-IR studies showed that the addition of MAM does not affect the structure of the cured epoxy. The mechanical properties of the blended system were studied systematically. The results demonstrated that the K_{IC} and impact strength at an MAM content of 10 phr for a toughened system increased by 91.5% and 83.5%, respectively, compared to those without MAM. But the tensile properties and flexural properties are reduced to some extent. The reason for the increase in fracture toughness and impact strength may be attributed to the nanophase structure obtained by self-assembly during the curing process. In addition, the toughness of the epoxy resin can be increased without significantly reducing the glass transition temperature. Therefore, amphiphilic block copolymer MAM could be used as an effective modifier to improve the mechanical properties of the epoxy resin without significantly reducing its thermal properties.

Author contributions

Conceptualization, Lei Tao, Zeyu Sun, and Muhuo Yu; data curation, Lei Tao; formal analysis, Chao Cheng; funding

acquisition, Muhuo Yu; investigation, Lei Tao, Wei Min and Hanwen Ou; methodology, Lei Tao and Zeyu Sun; supervision, Muhuo Yu and Zeyu Sun; software, Liangliang Qi; writing – original draft, Lei Tao.

Funding

This research was funded by the Shanghai Science and Technology Committee (project no. 17511102801 and 16DZ112140).

Conflicts of interest

There are no conflicts to declare.

References

1 K. Dong, J. Zhang, M. Cao, M. Wang, B. Gu and B. Sun, *Polym. Test.*, 2016, **55**, 44–60.
2 M. Pecora, Y. Pannier, M.-C. Lafarie-Frenot, M. Gigliotti and C. Guigon, *Polym. Test.*, 2016, **52**, 209–217.
3 X. Xiong, L. Zhou, R. Ren, X. Ma and P. Chen, *Polymer*, 2018, **140**, 326–333.
4 P. Vijayan P, D. Puglia, P. Vijayan P, J. M. Kenny and S. Thomas, *Mater. Technol.*, 2017, **32**, 171–177.
5 M. Wang, X. Fan, W. Thitsartarn and C. He, *Polymer*, 2015, **58**, 43–52.
6 J. Mijovic, M. Shen, J. W. Sy and I. Mondragon, *Macromolecules*, 2000, **33**, 5235–5244.
7 R. Konnola, J. Parameswaranpillai and K. Joseph, *Polym. Compos.*, 2016, **37**, 2109–2120.
8 X. Song and S. Xu, *J. Therm. Anal. Calorim.*, 2016, **123**, 319–327.
9 J. Zhang, Y. Wang, X. Wang, G. Ding, Y. Pan, H. Xie, Q. Chen and R. Cheng, *J. Appl. Polym. Sci.*, 2014, **131**, 378–387.
10 D. Cho and J. H. Hwang, *Adv. Polym. Technol.*, 2013, **32**, 5153–5162.
11 S. Grishchuk, L. Sorochynska, O. C. Vorster and J. Karger-Kocsis, *J. Appl. Polym. Sci.*, 2013, **127**, 5082–5093.
12 M. A. Hillmyer, P. M. Lipic, D. A. Hajduk, K. Almdal and F. S. Bates, *J. Am. Chem. Soc.*, 1997, **119**, 2749–2750.
13 J. Mijovic, M. Shen, J. W. Sy and I. Mondragon, *Macromolecules*, 2000, **33**, 5235–5244.
14 Q. Guo, R. Thomann, W. Gronski and T. Thurn-Albrecht, *Macromolecules*, 2002, **35**, 3133–3144.
15 J. M. Dean, R. B. Grubbs, W. Saad, R. F. Cook and F. S. Bates, *J. Polym. Sci., Part B: Polym. Phys.*, 2003, **41**, 2444–2456.
16 S. Ritzenthaler, F. Court, E. Girard-Reydet, L. Leibler and J. Pascault, *Macromolecules*, 2003, **36**, 118–126.
17 S. Maiez-Tribut, J.-P. Pascault, E. R. Soulé, J. Borrajo and R. J. J. Williams, *Macromolecules*, 2007, **40**, 1268–1273.
18 P. Gerard, N. P. Boupat, T. Fine, L. Gervat and J. P. Pascault, *Macromol. Symp.*, 2007, **256**, 55–64.
19 R. Yu, S. Zheng, X. Li and J. Wang, *Macromolecules*, 2012, **45**, 9155–9168.
20 F. Meng, S. Zheng and T. Liu, *Polymer*, 2006, **47**, 7590–7600.
21 J. M. Dean, N. E. Verghese, H. Q. Pham and F. S. Bates, *Macromolecules*, 2003, **36**, 9267–9270.
22 H. Kishi, Y. Kunimitsu, J. Imade, S. Oshita, Y. Morishita and M. Asada, *Polymer*, 2011, **52**, 760–768.
23 P. Oyanguren, M. Galante, K. Andromaque, P. Frontini and R. Williams, *Polymer*, 1999, **40**, 5249–5255.
24 N. Tanaka, T. Iijima, W. Fukuda and M. Tomoi, *Polym. Int.*, 1997, **42**, 95–106.
25 W. Fan, L. Wang and S. Zheng, *Macromolecules*, 2008, **42**, 327–336.
26 R. J. Varley, J. Hodgkin and G. P. Simon, *Polymer*, 2001, **42**, 3847–3858.
27 Y. Wei, F. Zengli and S. Yishi, *Acta Mech. Sin.*, 1989, **5**, 332–342.
28 B. Francis, S. Thomas, J. Jose, R. Ramaswamy and V. L. Rao, *Polymer*, 2005, **46**, 12372–12385.
29 Y.-x. He, Q. Li, T. Kuila, N. H. Kim, T. Jiang, K.-t. Lau and J. H. Lee, *Composites, Part B*, 2013, **44**, 533–539.
30 J. Wang, Z. Xue, Y. Li, G. Li, Y. Wang, W.-H. Zhong and X. Yang, *Polymer*, 2018, **140**, 39–46.
31 R. Barsotti, T. Fine, R. Inoubli, P. Gerard, S. Schmidt, N. Macy, S. Magnet and C. Navarro, *Nanostrength® Block Copolymers for Epoxy Toughening*, Thermoset Resin Formulators Association, Illinois, 2008.

